Engineering Structures 294 (2023) 116629

Contents lists available at ScienceDirect

Engineering Structures

journal homepage: www.elsevier.com/locate/engstruct

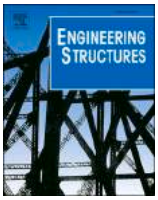

The role of a novel coating of SFRCR-ECC in enhancing the fire performance of CFST columns: Development, characteristic and ISO-834 standard fire test

Yan Xiong [a], Kairen Lin [b], Di Wu [c,*], Yuhong Ling [a], Solomon Tesfamariam [d]

[a] State Key Laboratory of Subtropical Building Science, South China University of Technology, Guangzhou, China
[b] School of Civil Engineering and Transportation, South China University of Technology, Guangzhou, China
[c] Engineering Research & Test Center, Guangzhou University, Guangzhou 510405, China
[d] Department of Civil and Environmental Engineering, University of Waterloo, 200 University Ave W, Waterloo, ON N2L 3G1, Canada

ARTICLE INFO

Keywords:
Spray-applied, fire-resistive and corrosion-resistive Engineered Cementitious Composites (SFRCR-ECC)
Fireproof coating
CFST
Fire resistance

ABSTRACT

The conventional spray-applied fire-resistive material meets the basic fire resistance requirements. However, it has limited strength and ductility, and poor bonding with the substrate, consequently, it will not deform with the main structure and reduces the fire resistance performance. A multifunctional spray-applied, fire-resistive and corrosion-resistive Engineered Cementitious Composites (SFRCR-ECC) has been developed to overcome these defects. Material properties of SFRCR-ECC coating were initially investigated, as well as the ISO-834 standard fire test of CFST columns sprayed with SFRCR-ECC coating were carried out. The effects of SFRCR-ECC coating thickness and the load ratio of the columns to the fire resistance limit were preliminarily explored, while the damage of the specimens after the open fire test, the temperature distribution and the axial deformation of CFST columns were obtained. The open fire test results also proved that SFRCR-ECC has excellent fire resistance performance as a new sprayable fire resistant material.

1. Introduction

Concrete-filled steel tube (CFST) columns utilize beneficial material properties of steel and concrete. They offer excellent performance under compression loads and contribute to ease of construction [1–4]. The outer steel tubes can also be used as a formwork for pouring concrete, which contribute to cost savings and speeding the construction process [5]. The CFST columns are widely used in high-rise and super-high-rise buildings [2,6], and fire safety must be investigated. In order to ensure and improve resistance of the fire safety level of civil buildings with heights greater than 250 m, the technical requirement provided by the Ministry of Public Security [7] specifies that the main load-bearing members must have high fire resistance performance, with the fire resistance limit of columns not less than four hours.

In the large load ratio or complex working conditions, CFST columns often need to be provided with fireproof coatings to meet the specified fire resistance limit. The fire performance of fireproofing coatings will be significantly degraded under natural weathering conditions, and the research on their weathering resistance and durability is emerging issues [8]. Kodur *et al.* [9,10] used a numerical method based on fracture mechanics to demonstrate crack initiation, extension and delamination of SFRM at the steel surface under seismic action [11] or impact loading [12]. They found that adding thickness of thermal insulation may not be the best solution to enhance the fire performance of steel structures [11]. It is worth mentioning that Naser *et al.* [13] used machine learning for structures and fire protection, including the CFST column database developed by Thai *et al.* [14]. Their sensitivity analysis showed that geometrical and dimensional characteristics are more significant to the mechanical response of CFST columns. Song *et al.* [15] conducted open-fire tests on CFST columns protected by fireproof coatings, and found that penetrating cracks in the coating can easily cause the coating to peel off or even fail. This resulted in rapid temperature rise and material deterioration, which reduces the fire resistance of CFST columns, with the thicker the coating, the greater the effect of cracks. Pessiki *et al.* [16,17] investigated the post-earthquake fire performance of the steel frame beam-column connection protected by SFRM and found that the

* Corresponding author.
E-mail addresses: xyan@scut.edu.cn (Y. Xiong), Tesfamariam@ubc.ca (K. Lin), wdzooo@sohu.com (D. Wu), yhling@scut.edu.cn (Y. Ling), solomon.tesfamariam@uwaterloo.ca (S. Tesfamariam).

https://doi.org/10.1016/j.engstruct.2023.116629

Available online 15 August 2023

Table 1
Mix proportions of SFRCR-ECC (kg/m^3).

Materials	Unit weight
Cement (C)	300
Fly ash (FA)	490
Fly ash cenosphere (FAC)	210
Silica sand	330
Water (W)	330
PE fiber (1.0%)	9.7
PP fiber (0.3%)	2.7
Water reducer (WR)	32
Thickener	0.5

damage of SFRM leads to heat transfer to the columns, which raised the temperature, significantly reduced the strength and stiffness, and impacted the load-bearing capacity. The aforementioned studies highlight that common fireproof coatings have low tensile and compressive strength, limited ductility and toughness, and poor bonding with anti-corrosion primer or substrate, under the action of environmental, seismic or impact load. The coatings will deform with the structure, as a result, there is a potential for large cracks or even spalling. This will contribute to the loss of the substrate protection, and fail to achieve to meet the service of the structure in the same cycle, which will increase the cost of subsequent coating maintenance and replacement.

Engineered Cementitious Composite (ECC) utilizes the principles of fracture mechanics and micromechanics to systematically design, adjust, and optimize the material system [18,19]. This will result in composites with a tensile strain rate of more than 3%, which is 300 to 500 times higher than that of ordinary concrete materials, using only 2% volume doping of fibers (e.g., polyethylene fibers), with a deformation capacity comparable to that of steel [20,21]. ECC materials have fine and multi-cracking properties and stable strain hardening state, while their crack width can be controlled below 50 μm [22,23], which can effectively resist the intrusion of corrosive media. Studies have shown that the chloride diffusion coefficient of ECC is only 50% of mortar and 10%-35% of concrete [24]. Meanwhile, ECC exhibited better mechanical properties, dimensional stability and lower erosion tendency than mortar in the simulated corrosive sewer environment [25]; after 420 days of exposure to be concentrated sulfate and sulfate chloride environments, ECC still possessed a significantly finer multi-crack development state, effectively retarding the deterioration process and providing better durability [26]. Thus, ECC is widely used in hydraulic, port, tunnel and bridge protection [27–32].

In recent years, a growing number of studies have shown that ECC can be used as a fire-resistant material [33–37]. Compared with traditional fireproof coatings, Fire-Resistive ECC (FR-ECC) has better bonding properties [33], and FR-ECC also combines thermal insulation properties, high-tensile strength and ductility, which can be an excellent solution for the problem of durability of traditional brittle fireproof coatings [34], ECC can as well overcome the deficiencies of large cracks and spalling that occur with ordinary thick fireproofing materials under environmental erosion, normal service loads, seismic loads, and impact loads [36,37]. Among them, Victor Li et al. [34] developed a sprayable SFR-ECC and characterized the bonding performance between ECC and still based upon the energy change of interfacial fracture, and the results showed that the SFR-ECC/steel interface exhibited a fiber-related toughness behavior across the fracture with excellent bonding performance. However, the added latex bonding agent does not have excellent thermal stability, and the cohesive properties at high temperatures will be reduced, so its bonding method still needs to be improved. Cai et al.

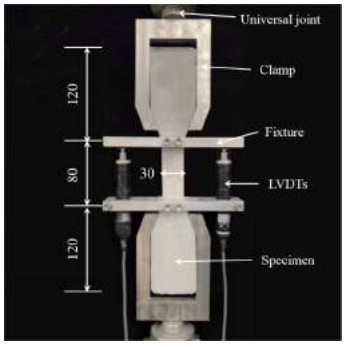

(a) Tensile test

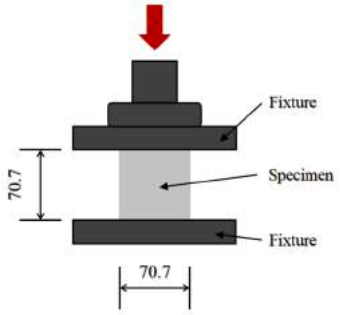

(b) Compressive test

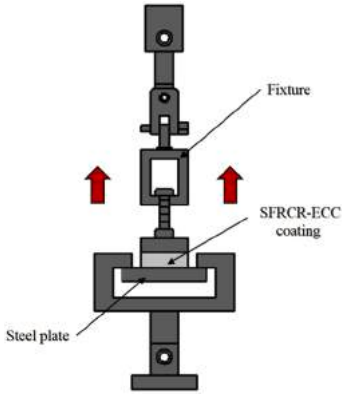

(c) Adhesive test

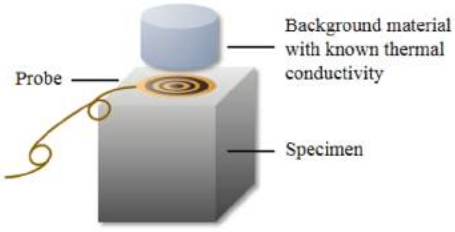

(d) Thermal parameter test

Fig. 1. Specimen and test setup.

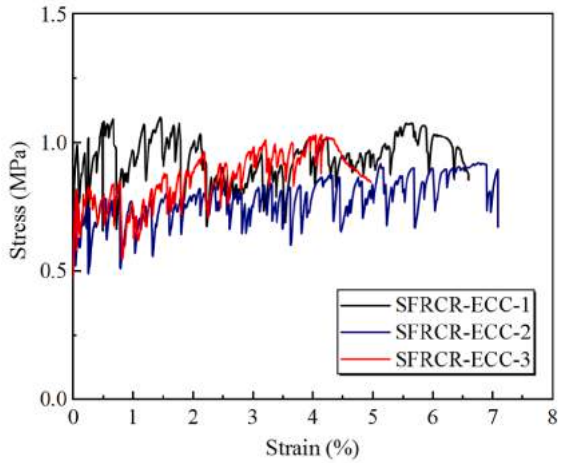

(a) Tensile stress-strain curves

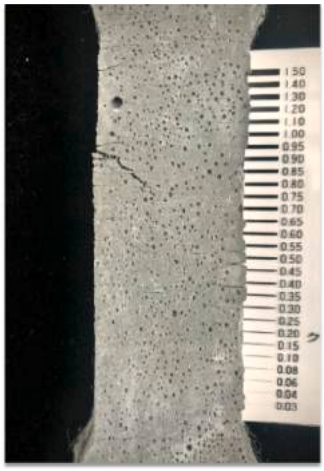

(b) Multiple microcracks

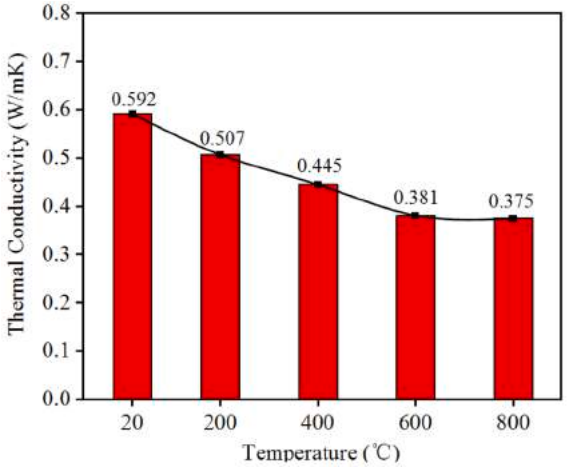

(c) Thermal conductivity

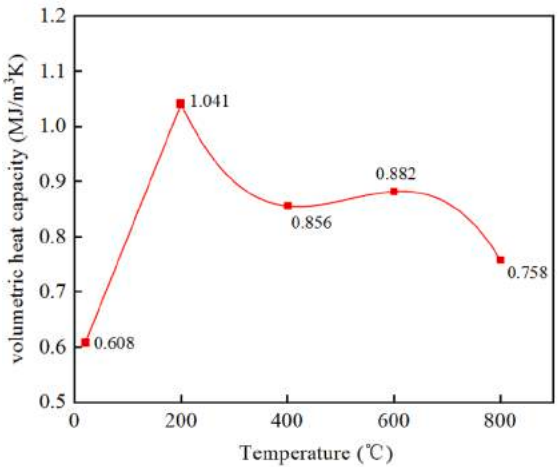

(d) Volumetric heat capacity

Fig. 2. Material properties of SFRCR-ECC.

Table 2
Mechanical and thermal properties of SFRCR-ECC.

Dry density (kg/m^3)	Tensile strength (MPa)	Tensile strain (%)	Compressive strength (MPa)	Bonding strength (MPa)	Thermal conductivity (W/m k)
1317	1.02	5.91	9.15	0.71	0.592

[37] developed a new type of FR-ECC to be used as a fireproof coating for steel beams and carried out a study on the fire resistance of post-earthquake steel beams protected by FR-ECC. Their results showed that the FR-ECC maintained the integrity after cyclic loading, its fine and multi-cracking characteristics and molten fibers relieve the thermal stress concentration between FR-ECC and steel substrate, slow down the heating rate, and enable the steel beams protected by FR-ECC to exhibit better fire resistance limits. The pre-treatment entailed polishing the substrates and brushing the binder materials, so the convenience of construction and the high-temperature resistance of the binder materials needs to be improved.

Fly ash cenosphere (FAC) is a kind of hollow spherical particle extracted from fly ash, which is light and high-temperature resistant. It is often added to the cement matrix as an artificial defect with the aim of reducing the density and thermal conductivity of the material [38]. Addition of FAC resulted in better fiber dispersion, and the spherical

Table 3
Detailed parameters of specimens.

Specimen	Outer diameter (mm)	Wall thickness (mm)	Column height (mm)	Steel tube	Concrete	SFRCR-ECC thickness (mm)	Loadratio	Testload (kN)	Firesituation
Z1C1-40	325	10	3770	Q355B	C50	40	0.42	2609	four-side fire
Z1C2-30	300	18				30	0.42	3321	
Z2C2-40	300	18				40	0.59	4558	

Fig. 3. CFST columns for open fire test.

surface reduced the curvature of the fracture paths between the mortar interfaces in order to achieve the effect of reducing the crack development [39]. FAC, as industrial waste, is in line with the concept of green building materials and is worthy of further exploration.

In this study, a multifunctional version of spray-applied, fire-resistive and corrosion-resistive Engineered Cementitious Composites (SFRCR-ECC) has been developed incorporating FAC and PP fibers. FAC is used to reduce density and thermal conductivity, and PP fiber is used to avoid bursting of the coating at high temperatures. Without any binder, SFRCR-ECC is sprayed directly onto the surface of steel members under a certain pressure. SFRCR-ECC combines the multifunction of both a fireproof coating and an anti-corrosion coating, and achieves a good bonding with the surface of steel structure.

The technology will be applied to the Guangzhou Baiyun Railway Station Integrated Transportation Hub Project and the Guangzhou Knowledge Tower Project, a super high-rise building. This study was carried out for the new Baiyun railway station project in Guangzhou to study the fire resistance performance of reduced scale round CFST columns after spraying SFRCR-ECC, the effects of coating thickness, load ratio, and thickness of steel tube on fire resistance performance of CFST columns were initially explored.

2. Characteristic of protective coating

2.1. Mixtures and test setup of protective coating materials

The constituent materials used for SFRCR-ECC in this study include cement, fly ash, fly ash cenosphere, silica sand, polyethylene (PE) fiber, polypropylene (PP) fiber, and water. Among them, fly ash as an industrial waste improves the greenness of the coating, while FAC reduces the density and thermal conductivity [38]. PE fiber (1.0% by volume) of 25 μm diameter and 12 mm length has an elastic modulus of 116 GPa and a tensile strength of 2.9 GPa to increase the ductility of the coating [40]; PP fiber (0.3% by volume) of 32 μm diameter and 12 mm length has an elastic modulus of 4 GPa and a tensile strength of 0.4 GPa to avoid bursting at high temperatures [41,42]. Water reducer (WR) and thickener are adjusted to improve the workability and spraying performance of the coating. The mechanical properties, thermal insulation performance, spraying process and construction performance tests of SFRCR-ECC specimens with different mix ratios were carried out in the previous phase, and the best mix proportions of SFRCR-ECC were finally selected as shown in Table 1.

Dog bone specimens (Fig. 1a) according to [43] were prepared to characterize the uniaxial tensile performance of SFRCR-ECC at 28 days. The loading rate was 0.5 mm/min. Two linear variable displacement transducers (LVDTs) were externally mounted on both sides of the specimen with a hoop to measure the deformation of the central 80 mm gauge segment. The compressive strength of SFRCR-ECC was obtained by 70.7 mm cube specimens at 28d (Fig. 1b). The loading rate was 0.5 mm/min. The bonding strength test of SFRCR-ECC with steel substrate is according to [44] (Fig. 1c), and the loading rate was 0.2 mm/min. The thermal conductivity test is conducted according to [45], using a Hot Disk thermal constant analyzer (Fig. 1d), to determine the thermal parameter of 70.7 mm cubic specimens after experiencing high temperature effects at 20 °C, 200 °C, 400 °C, 600 °C, and 800 °C.

2.2. Properties test results of SFRCR-ECC coating

It can be seen that all SFRCR-ECC specimens exhibit strain-hardening and multiple cracks (Fig. 2a). The average tensile strength is 1.02 MPa and the average ultimate tensile strain rate is 5.91%, which exhibit good ductility. The specimens show fine and multi-cracking development, and the crack widths are mostly below 50 μm (Fig. 2b), which can obstruct the intrusion of harmful ions and flames as well as enhance the corrosion and fire resistance of the substrates. The average compressive strength of SFRCR-ECC is 9.15 MPa, which is about five times that of conventional cementitious fire-resistive material. The average bond strength of SFRCR-ECC is 0.71 MPa, which is 17.7 times higher than the 0.04 MPa required by the code [44], reflecting a better bond performance. It is worth mentioning that no external bonding agent is used between the coating and the steel plate. Fig. 2c illustrates the thermal conductivity test results of SFRCR-ECC in the range of 20 to 800 °C. As the temperature increases, the thermal conductivity of the coating decreased and eventually plateaus at 600 to 800 °C. While Fig. 2d shows the volumetric specific heat capacity test results of SFRCR-ECC in the range of 20 to 800 °C. With the temperature increasing, volumetric specific heat capacity peaked at 200 °C and subsequently decreased. As evaporation of combined water and decomposition of hydration products consume energy, the specific heat capacity increases. However, increase in porosity will reduce the specific heat capacity. Consequently, due to the combined effect, the volume specific heat capacity - temperature curve shows a fluctuating trend.

It has been noted that SFRM materials have an ultimate tensile strength of less than 0.1 MPa and a strain capacity of only 0.01% [34]. The SFRCR-ECC, however, has a tensile strength of 1.02 MPa and an ultimate tensile strain rate of 5.91%, resulting in better tensile properties compared to SFRM materials. Li *et al.* [34], through bonding performance tests, found that SFR-ECC is better attached to steel substrates, whereas SFRM materials exhibit a brittle failure mode. Therefore, the mechanical properties of SFRCR-ECC are superior to that of conventional SFRM materials.

2.3. Material properties of SFRCR-ECC coating

According to the test results in section 2.2, material properties of SFRCR-ECC are provided in Table 2.

Table 4
Mix proportions of concrete (Unit: kg/m^3).

Strength level	Water binder ratio	Water	Cement	Coarse aggregate	Fine aggregate	Fly ash	Mineralpowder	Water reducing agent
C50	0.29	140	333	1094	643	58	92	14.48

(a) Loading concrete into the funnel

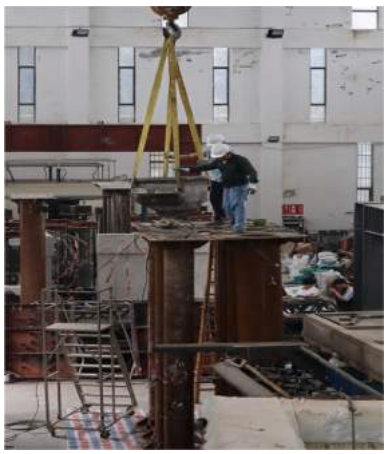

(b) Pouring core concrete

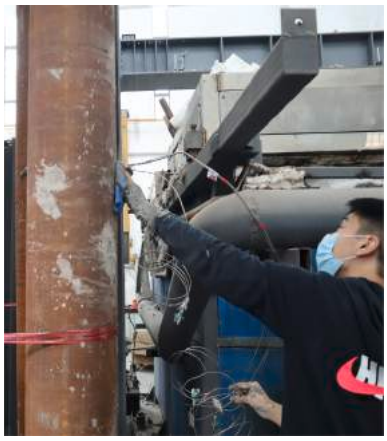

(c) Positioning thermocouples

(d) Casting cube specimens

(e) Spraying SFRCR-ECC

(f) Smoothing column surface

(g) Measuring coating thickness

(h) Enlarged view of coating thickness

Fig. 4. Images of specimen production.

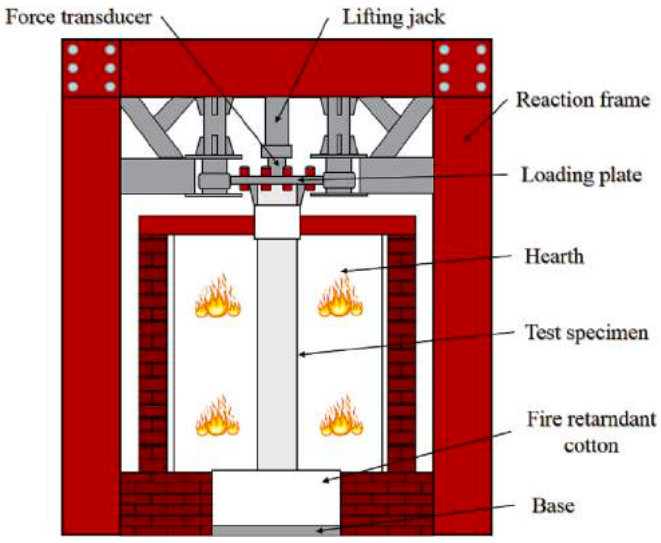

Fig. 5. The furnace for vertical structure elements.

3. ISO-834 standard fire test

3.1. Fire test preparation

3.1.1. Specimen design

SFRCR-ECC will be applied to the fire and corrosion prevention of CFST columns in the second phase of the new Guangzhou Baiyun Railway Station Project (hereinafter referred to as Baiyun Station Project). Therefore, three specimens made in this test were designed according to the actual size of CFST columns in Baiyun station project by scaling down. The load ratio of the most unfavorable condition in Baiyun station project is 0.42, so the load ratios of our test specimens are selected as 0.42 and 0.59 (the maximum loading capacity of the furnace for vertical structure elements in the laboratory), respectively. Detailed dimensions and parameters of the specimens are provided in Table 3, and the CFST columns are shown in Fig. 3.

3.1.2. Material properties

The steel tube of the specimens is made of Q355B grade steel with a yield strength of 405 MPa. The core concrete of CFST tested is C50 commercial concrete, the concrete mix proportions are provided in Table 4.

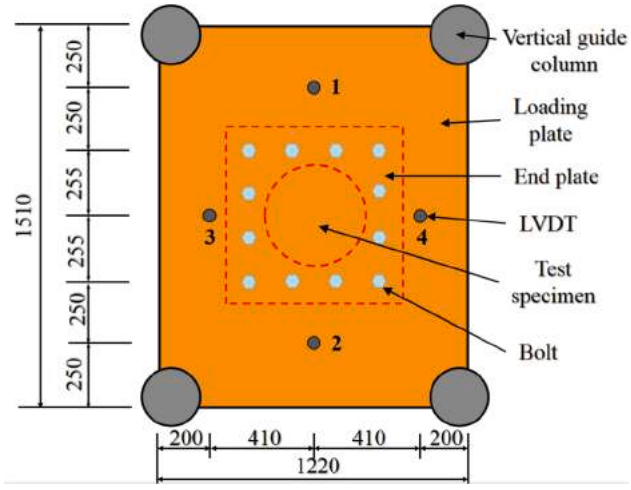

(a) Arrangement of LVDTs

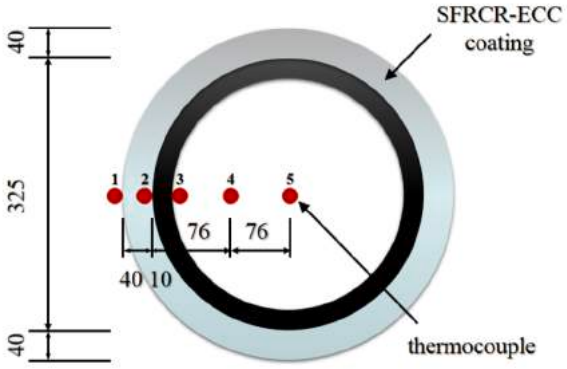

(b) Z1C1-40

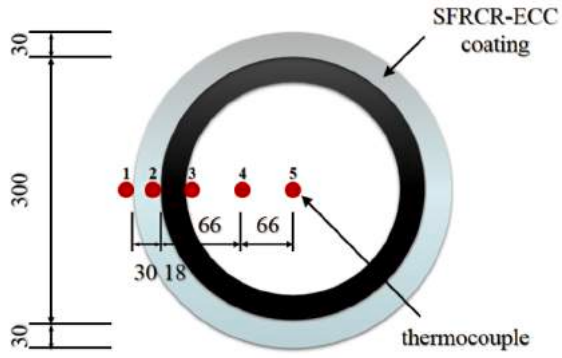

(c) Z1C2-30

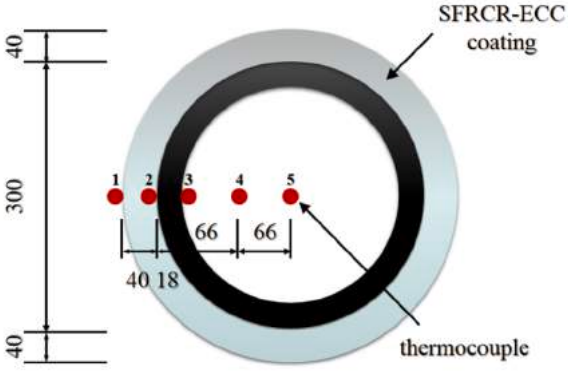

(d) Z2C2-40

Fig. 6. Arrangement of thermocouples and LVDTs (unit: mm).

Fig. 7. Fire protection treatment of specimen.

3.1.3. Specimen production

The specimen production is carried out in the following order:

- the first step, the commercial concrete is loaded into a specially designed large funnel (Fig. 4a) for subsequent pouring from overhead;
- the second step, the core concrete is poured from the hole on the end plate of the column and vibrated evenly with an immersion vibrator (Fig. 4b), and when it is poured to the half-height section of the column, a bundled thermocouple is inserted through the air hole and kept it fixed (Fig. 4c);
- the third step, pour a number of cubic specimens and cylindrical specimens (Fig. 4d), which can be tested for compressive strength;
- the fourth step, the holes on the end plate of the columns are sealed after the core concrete has hardened;
- the fifth step, spray SFRCR-ECC on the column surface until the thickness of the coating reaches the set value (Fig. 4e);
- the sixth step, the uneven surface of the coating is smoothed with mortar (Fig. 4f), aiming to avoid causing errors.
- Finally, the thickness of the coating is measured (Fig. 4g-h). The specimen fabrication process is shown in Fig. 4.

To achieve the objective of not using any binder and maintaining good bonding of the protective coating with the surface of steel structure, a version of spray-applied protective coating materials has been developed in this study. As a more ideal coating construction process at the present, spraying reduces the cost and time of making formwork and realizes construction over large areas, which can effectively improve the efficiency. Xu et al. [46] conducted a study of the interfacial bonding behaviors between sprayed UHTCC and concrete substrate, which showed that the spraying needs to satisfy the two-stage characteristics, i.e., the rheology of the pumping process and the cohesiveness of the spraying process. The team used wet sprayed UHTCC to strengthen reinforced concrete beams, and the study showed that the sprayable UHTCC layer can effectively control cracks in the concrete layer and improve the durability of the structure [28,47]. In this study, SFRCR-ECC was used to protect the round CFST columns, and two different protection thicknesses of 30 mm and 40 mm were selected.

(a) Before the fire test

(b) After the fire test

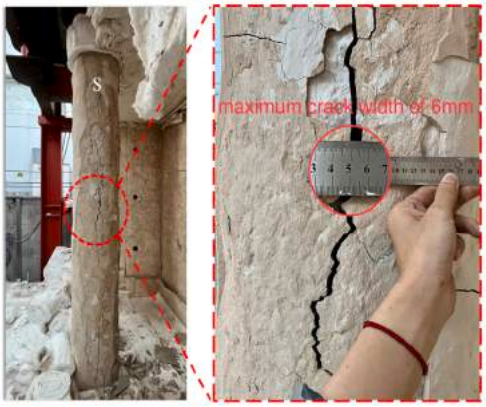

(c) Spalling on the south side of the specimen and the maximum crack width

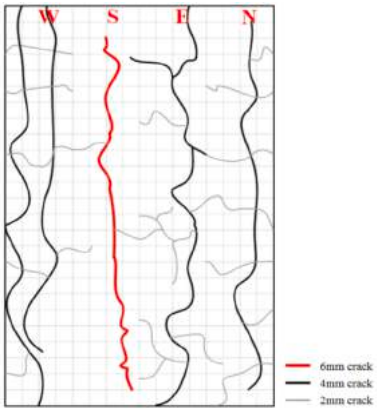

(d) Expanded view of coating damage after 210 minutes of high temperature

Fig. 8. Specimen Z1C1-40 after fire test.

3.1.4. Fire test setup

The CFST columns were exposed to ISO 834 fire in the furnace for vertical structure elements of the Structural Fire Resistance Laboratory in South China University of Technology. The working dimension of furnace chamber is 2.5 m × 2.5 m × 3 m, with a loading capacity of 500 tons. The test setup is shown in Figs. 5 and 7.

The overall axial deformations of the column specimens were measured by 4 LVDTs arranged on the loading plate at the top of the column. The temperature at different locations in the same section of each specimen were monitored by five thermocouples placed at half-height sections of the specimen during the fire exposure. The specific arrangement of the displacement transducers and thermocouples is shown in Fig. 6.

Before the open fire test, the upper and lower ends of the specimen are wrapped in fireproof cotton within 385 mm to ensure that the actual height of the specimen under fire is about 3 m. The fireproof treatment of the specimen is shown in Fig. 7.

3.1.5. Failure criteria

"Determination Guidelines" of "Fire-resistance tests—Elements of building construction—Part 1: General requirements" (GB/T 9978.1-2008) [48], the parameters for determining the load capacity of the specimen during the fire resistance test are the axial deformation of the column reaches -H/100 (i.e. the average displacement value of LVDTs reaches −37.7 mm); the rate of change of the column axial deformation reaches -H/300 per min (i.e. −10 mm/min); the vertical load drops sharply and the jack cannot continue to be maintained at the set load.

3.2. Fire test phenomenon

3.2.1. Specimen Z1C1-40

After 210 min of ignition, the specimen was still in the expansion phase, but also stable to withstand the predetermined axial pressure, as the specimen had reached the first level of refractory limit, while considering the vertical fire test furnace was approaching the safe burning time limit, the test was terminated.

After the test, when the specimen was cooled to room temperature and the furnace was opened, it was observed that the coating surface was light yellowish gray, and some blocks showed light pink color (Fig. 8b and Fig. 8c). There was a little spalling on the south side of the specimen, with the maximum spalling depth of 5 mm, and several long cracks appeared on the surface of the coating (Fig. 8c). The longest crack length is 800 mm, and the maximum crack width is about 6 mm. There was no bulging and bending around the specimen. The failure model of the specimen is shown in Fig. 8.

3.2.2. Specimen Z1C2-30

Since the test began, the specimen Z1C2-30 was heated and expanded, with the pressure gauge reading rising slowly, adjusting the oil pressure of the hydraulic jack continuously during the test in order to maintain the same axial pressure. In the process of the test, water vapor overflowed above the loading plate. After 210 min of ignition, the specimen was still in the expansion stage, but also withstood the pre-determined axial pressure. As the specimen reached the first level of refractory limit, as well as consideration of the vertical fire test furnace

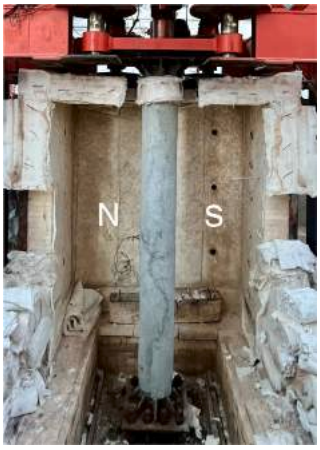

(a) Before the fire test

(b) After the fire test

(c) A little spalling on the surface

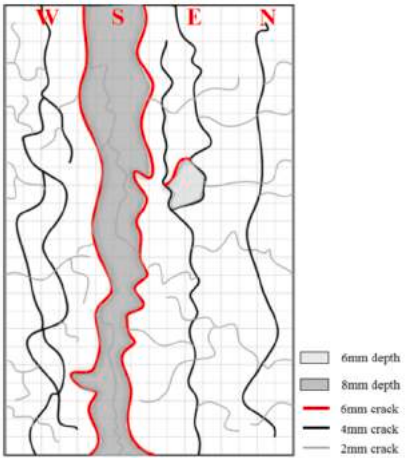

(d) Expanded view of coating spalling and cracking after 210 minutes of high temperature

Fig. 9. Specimen Z1C2-30 after fire test.

approached the safe burning time limit, the test was terminated.

After the fire test, the specimen was cooled to room temperature, and the furnace was opened. The color change of the coating of specimen Z1C2-30 is similar to that of the coating of specimen Z1C1-40 (Fig. 9b and Fig. 9c).There was a little spalling on the surface of the coating on the south side of the specimen, with the maximum spalling depth of 8 mm (Fig. 9c); a certain quantity of small crack without distribution pattern appeared on the surface of the coating, with the maximum crack width of 6 mm; the specimen did not appear bulging or bending phenomenon. The failure model of specimen Z1C2-30 is shown in Fig. 9.

3.2.3. Specimen Z2C2-40

After the test starts, specimen Z2C2-40 was heated and expanded, while the pressure transducer gauge reading rising slowly. For ensuring that the specimen was subjected to constant axial pressure during the test, the oil pressure of the hydraulic jack required constant adjustment. During the test, water vapor can be observed overflowing from above the loading plate. After 210 min of ignition, the specimen was in the expansion stage and could still steadily withstand the predetermined axial pressure. As the specimen had reached the first level of refractory limit, while considering the vertical fire resistance test furnace was close to the safe burning time limit, the fire test was terminated.

After the fire test, when the specimen was cooled to room temperature and the furnace was opened, it could be observed that the coating was light yellowish gray after the fire, and the spalling area showed light pink color (Fig. 10b and Fig. 10c). The southwest side of the specimen appeared a certain area of spalling, with a maximum spalling depth of 10 mm (Fig. 10c), while a number of irregularly distributed cracks occurred on the surface of the coating, with a maximum crack width of 6 mm; however, the specimen did not appear bulging and bending deformation. The failure model of specimen Z2C2-40 is shown in Fig. 10.

3.3. Temperature field analysis

3.3.1. Temperature rise curve measured in the furnace

During the test, the average temperature change inside the furnace was controlled according to the ISO-834 standard heating curve. Fig. 11. shows the comparison of measured temperature-burning time curves in furnace of the three specimens with the ISO-834 standard heating curve. As can be seen from the figure, the measured heating curves of the three specimens matches well with the standard heating curve in general, in which Z2C2-40 specimen is exposed to fire for 150 min, because one of the injectors in the refractory test furnace failed to ignite successfully, causing the temperature in the furnace to be 30 ~ 35 °C lower than the ISO-834 standard heating curve since 150 min.

3.3.2. Temperature field distribution of the specimens

The temperature–time curves of 5 measured points during the test of specimens Z1C1-40 to Z2C2-40 are shown in Fig. 12. From Fig. 12, it can be highlighted that:

(a) Before the fire test

(b) After the fire test

（c）Spalling of the coating

（d）Expanded view of coating spalling and cracking after 210 minutes of high temperature

Fig. 10. Specimen Z2C2-40 after fire test.

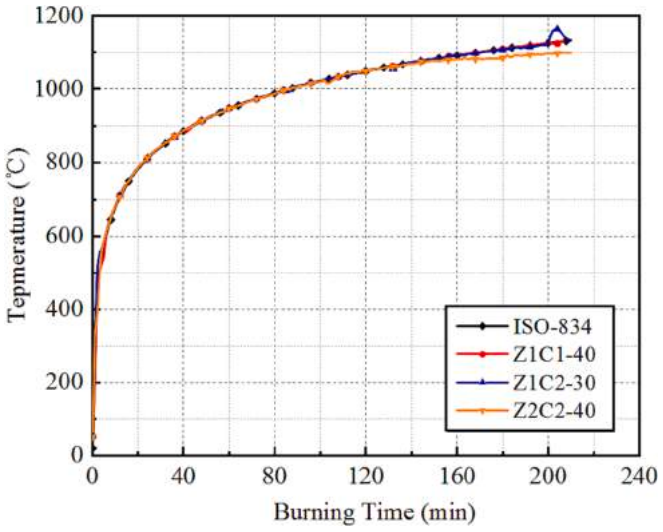

Fig. 11. Comparison of measured temperature-burning time curves in furnace and ISO 834 standard curve.

1. The temperature of each measurement point of the three specimens increased with the growth of the burning time, while the measured temperature progressively decreased with the depth of the points in the section at the half-height of the column. The temperature curve of the points located inside the concrete has the same trend, with an obvious temperature plateau in the range of 100 ~ 150 °C, which is due to the evaporation of water and heat absorption in the concrete; the duration of the temperature plateau of measurement point 5 is longer than that of measurement point 3, which is because the further the location of the points from the fire surface, the longer the water vapor escape path, requiring more time.
2. The temperature of point 1 of specimen Z1C1-40 displays a rising trend of rapid and then slow, which is similar to the furnace temperature rise rule. The temperature difference between points 1 and 2 indicates the thermal insulation of SFRCR-ECC coating, the temperature of the outer surface of the steel tube at point 2 is slow, while the temperature at the moment of 206 min is only 411 °C, at this moment SFRCR-ECC coating isolated 740 °C, which makes the steel tube does not have obvious loss of carrying capacity, and still can withstand the predetermined load stably, indicating that SFRCR-ECC coating shows good thermal insulation and certain thermal stability, which can significantly improve the fire resistance limit of the column. The temperature difference between point 2 and point 3 is that of the steel tube-concrete interface, which shows a tendency to rise

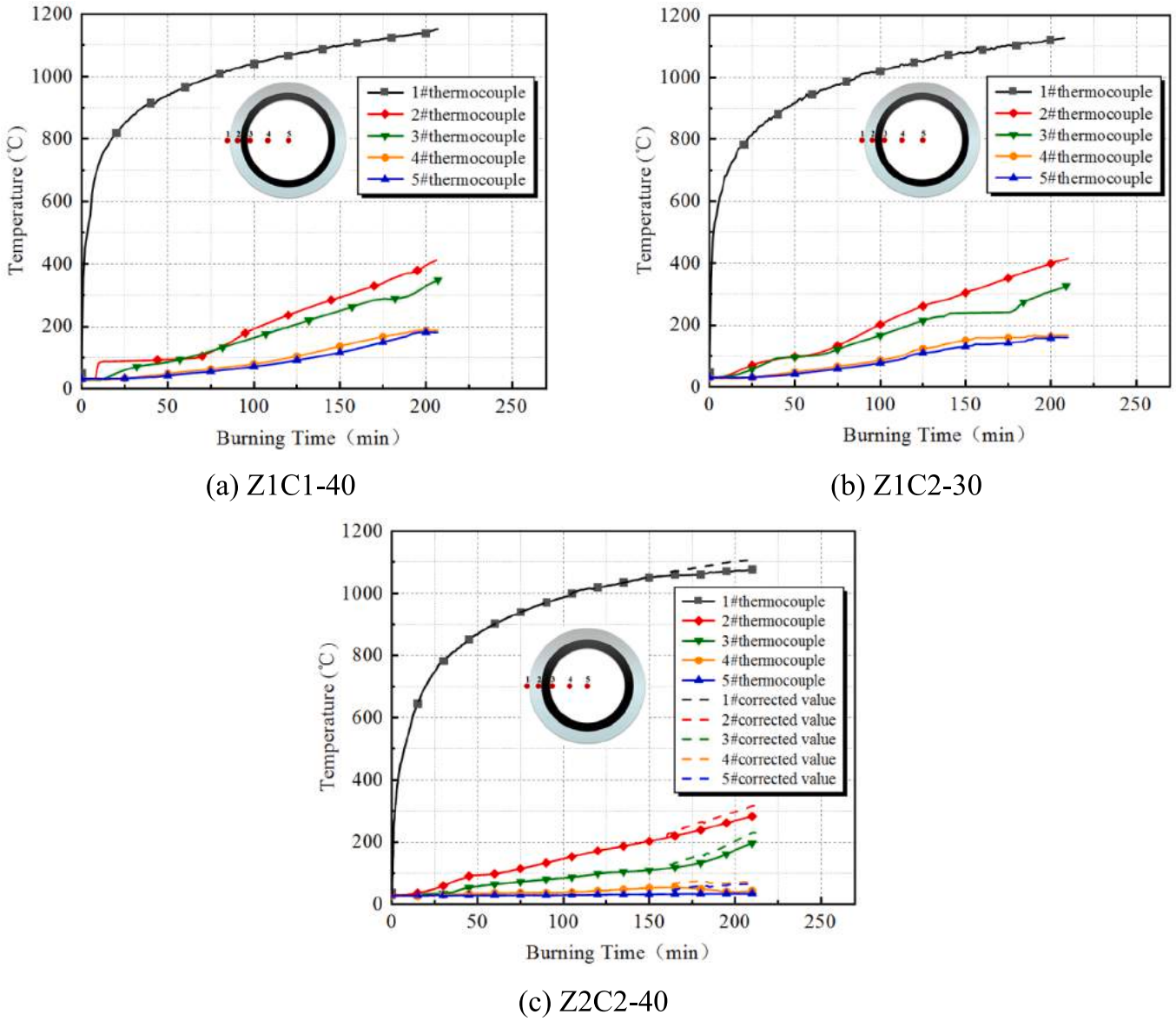

Fig. 12. Temperature-time curves.

and then fall with the burning time. This is mainly because the internal concrete may shrink during the curing period, resulting in a gap between the interface, which in turn generates the interface thermal resistance; At the beginning, as the steel tube heating rate is faster than the concrete, it expands first, and increases the gap between the interfaces, resulting in a rise in the interface temperature difference; as the burning time reaches 170 min, the internal concrete is heated to produce expansion, while under the action of vertical load, the lateral deformation of the core concrete will also increase, which further shortens the gap between the steel tube-concrete interface, causing a decrease in the interface temperature difference. Points 4 and 5 show a similar and more gentle warming trend, at 206 min, the temperature of core concrete point 5 is only 180 °C.

3. The temperature rise at points 1 to 5 of specimen Z1C2-30 is approximately the same as that of specimen Z1C1-40, except that the temperature difference at the steel tube-concrete interface of Z1C2-30 is larger than that of Z1C1-40, which is due to the wall thickness of the steel tube of section C2 is 18 mm, whereas the wall thickness of the steel tube of section C1 is 10 mm, Reflecting the temperature gradient of the inner and outer wall of the steel tube increases with the increase of the wall thickness; When the burning time reaches 208 min, the temperature difference between points 1 and 2 is 715 °C, at the moment the temperature of the outer wall of the steel tube is only 411.8 °C, so the mechanical properties of the steel tube are still well maintained, which is due to the good thermal insulation properties of SFRCR-ECC; the temperature difference of the steel tube - concrete interface still follows the trend of increasing and then decreasing with the burning time; The internal concrete points 4 and 5 also maintain the same relatively smooth rising trend, at 210 min, the temperature of core concrete point 5 is only 160 °C. It is worth mentioning that the 30 mm thick SFRCR-ECC coating can also meet the first level of fire resistance limit (180 min fire resistance limit), providing the possibility of cost optimization.
4. Due to the vertical fire resistance test furnace flamethrower failed to successfully ignite the ninth flame, resulting in the test piece Z2C2-40 temperature of each measurement point was reduced. At 210 min, the temperature of point 1 is only 1076 °C, about 75 °C less than the previous two specimens; the temperature difference between points 1 and 2 is 794 °C, at the moment the temperature of the outer wall of the steel tube is only 282 °C, almost no change in the mechanical properties of the steel tube, reflecting the excellent thermal

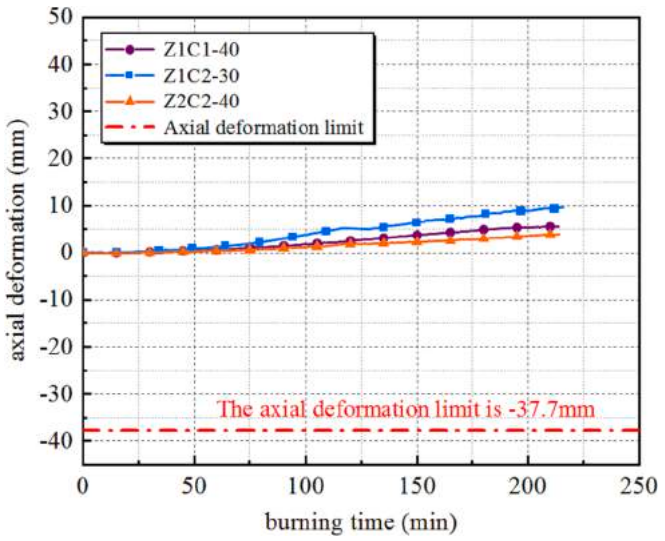

Fig. 13. Axial displacement-time curves of specimens.

insulation properties of SFRCR-ECC coating; In the meantime, the temperature difference at the interface of steel tube - concrete also follows the trend of rising and then falling with the burning time; the concrete internal measured points 4 and 5 keep a more stable trend, when 210 min, the temperature of core concrete measured point 5 is only 34.2 °C. Figure 20(c) provides the temperature corrected values of each measurement point of specimen Z2C2-40 after 150 min, reaching 210 min with a temperature corrected value of 316.12 °C for the outer wall point 2 of the steel tube, and 68 °C for the core concrete point 5.

3.4. Axial deformation analysis

The measured axial displacement–time curves obtained in the fire test are shown in Fig. 13. The curves involve only one stage, the expansion stage, but not compressive deformation stage or destruction stage. And the heat elongation deformation was always larger than compressive deformation due to the temperatures of the steel tubes with SFRCR-ECC coating were below 420 °C. As shown by the test results:

1. The variation of the axial displacement of the three samples with time was basically similar. The axial displacements of three samples increased with the elevated temperature throughout the open fire test process. A short fluctuation in axial deformation of specimen Z1C2-30 was found at about 120 min, probably due to cracks in the coating or expansion of the steel tube.
2. After 210 min, specimen Z1C1-40 reached a maximum expansion deformation of 5.56 mm; specimen Z1C2-30 reached a maximum expansion deformation of 9.45 mm; specimen Z2C2-40 reached a maximum expansion deformation of 3.86 mm. It can be seen that as the thickness of SFRCR-ECC coating decreased, the deformation of the specimen increased for the same fire time and the thermal elongation deformation of the specimen became steeper with time; as the axial compression ratio increased, the deformation of the specimen decreased for the same fire time and the thermal elongation deformation of the specimen becomes flatter with time.
3. During the 210 min fire test, three specimens were exposed to four-sides fire, with the deformation of the specimens at the expansion stage and no compressive deformation, while the deformation value did not reach the failure limit of the column bearing capacity, indicating that the fire resistance of the three specimens was excellent and the fire resistance limits of all three specimens were well over 180 min.

4. Summary and conclusions

To avoid the inherent brittleness, low cohesion and poor durability of conventional SFRM, a novel multifunctional version of spray-applied, fire-resistive and corrosion-resistive Engineered Cementitious Composites (SFRCR-ECC) was developed and used as the thermal and environmental barrier coating for CFST columns. The temperature field distribution, axial deformation development, fire resistance and failure mode of 3 CFST columns sprayed with SFRCR-ECC coatings under fire were experimentally determined and compared. The following conclusions can be drawn:

1. SFRCR-ECC specimens exhibited good strain-hardening properties and multiple microcracking behaviors during tensile processes. The average tensile strength is 1.02 MPa and the average ultimate tensile strain rate is 5.91%. The crack widths of specimens are mostly below 50 μm.
2. SFRCR-ECC coating experiences milder damage under fire due to micro-cracks, melted fibers in SFRCR-ECC and good bonding properties between the coating and the tube wall. Some specimens have a little spalling of the outer surface layer of the coating, the depth of spalling is 6 ~ 10 mm; some specimen has irregular and fine cracks, with crack widths of 2 ~ 6 mm.
3. SFRCR-ECC as a protective coating had excellent thermal insulation performance. After fire test lasted 210 min, the temperature of the outer wall of the CFST specimen with the SFRCR-ECC coating thickness of 30 mm was 415 °C, the temperature of the inner wall of the steel tube was 330 °C, the core concrete temperature was only 160 °C.
4. During the fire test, all 3 specimens coated by SFRCR-ECC were in the uncompressed expansion stage. When the load ratio was 0.42, the axial elongation of specimen Z1C1-40 and Z1C2-30 were 5.56 mm and 9.45 mm, respectively; when the load ratio was 0.59, the axial elongation of specimen Z2C2-40 was 3.86 mm. The fire resistance limit of all 3 specimens had reached 210 min, which satisfied the first grade of fire resistance as stipulated in the ''Code for Fire Protection in Building Design''.

Compared to conventional SFRM, SFRCR-ECC is expected to be a durable alternative to current SFRM due to its higher mechanical, sprayability, bondability and low thermal conductivity.

CRediT authorship contribution statement

Yan Xiong: Conceptualization, Methodology, Writing – review & editing. **Kairen Lin:** Investigation, Data curation, Writing – original draft. **Di Wu:** Conceptualization, Project administration, Investigation, Writing – review & editing. **Yuhong Ling:** Conceptualization, Validation. **Solomon Tesfamariam:** Writing – review & editing.

Declaration of Competing Interest

The authors declare that they have no known competing financial interests or personal relationships that could have appeared to influence the work reported in this paper.

Data availability

Data will be made available on request.

Acknowledgments

The authors are thankful for the support from National Natural Science Foundation of China (52278501, 51878298), Natural Science Foundation of Guangdong Province (2021A1515012606), Guangdong Provincial Key Laboratory of Modern Civil Engineering Technology

(2021B1212040003).

References

[1] Zeghiche J, Chaoui K. An experimental behaviour of concrete-filled steel tubular columns. J Constr Steel Res 2005;61(1):53–66. https://doi.org/10.1016/j.jcsr.2004.06.006.

[2] Han LH, Li W, Bjorhovde R. Developments and advanced applications of concrete-filled steel tubular (CFST) structures: members. J Constr Steel Res 2014;100:211–28. https://doi.org/10.1016/j.jcsr.2014.04.016.

[3] Guo L, Liu Y, Fu F, et al. Behavior of axially loaded circular stainless steel tube confined concrete stub columns. Thin-Walled Struct 2019;139:66–76. https://doi.org/10.1016/j.tws.2019.02.014.

[4] Li M, Yao L, He L, et al. Experimental study on the compressive behavior of concrete filled steel tubular columns with regional corrosion//Structures. Elsevier. 2022, 35: 882-892. https://doi.org/10.1016/j.istruc.2021.11.060.

[5] Shao Z, Zha X, Wan C. Design method of fire-resistance capacity of reinforced-concrete-filled steel tube column under axial compression. Fire Saf J 2022;129:103572. https://doi.org/10.1016/j.firesaf.2022.103572.

[6] Zhong S-T, Zhang S. Application and development of concrete-filled steel tubes (CFST) in high rise buildings. Adv Struct Eng 1999;2(2):149–59. https://doi.org/10.1177/136943329900200207.

[7] Gongxiao [2018] No. 57. Enhanced technical requirements for fire protection design of civil buildings with building heights greater than 250m (Trial). Beijing: Ministry of Public Security of the People's Republic of China; 2018.

[8] Anees SM, Dasari A. A review on the environmental durability of intumescent coatings for steels. J Mater Sci 2018;53:124–45. https://doi.org/10.1007/s10853-017-1500-0.

[9] Kodur V, Arablouei A. Effective properties of spray-applied fire-resistive material for resistance to cracking and delamination from steel structures. Constr Build Mater 2015;84:367–76. https://doi.org/10.1016/j.conbuildmat.2015.03.022.

[10] Arablouei A, Kodur V. Cohesive zone model properties for evaluating delamination of spray-applied fire-resistive materials from steel structures. Eng Fract Mech 2015;143:138–57. https://doi.org/10.1016/j.engfracmech.2015.06.037.

[11] Arablouei A, Kodur V. A fracture mechanics-based approach for quantifying delamination of spray-applied fire-resistive insulation from steel moment-resisting frame subjected to seismic loading. Eng Fract Mech 2014;121:67–86. https://doi.org/10.1016/j.engfracmech.2014.03.003.

[12] Arablouei A, Kodur V. Dynamic delamination of fire insulation applied on steel structures under impact loading. Int J Impact Eng 2015;83:11–27. https://doi.org/10.1016/j.ijimpeng.2015.04.006.

[13] Naser MZ, Kodur V, Thai HT, et al. StructuresNet and FireNet: benchmarking databases and machine learning algorithms in structural and fire engineering domains. J Build Eng 2021;44:102977. https://doi.org/10.1016/j.jobe.2021.102977.

[14] Naser MZ, Thai S, Thai HT. Evaluating structural response of concrete-filled steel tubular columns through machine learning. J Build Eng 2021;34:101888. https://doi.org/10.1016/j.jobe.2020.101888.

[15] Song QY, Han LH, Zhou K, et al. Fire resistance of circular concrete-filled steel tubular (CFST) column protected by intumescent coating. J Constr Steel Res 2018;147:154–70. https://doi.org/10.1016/j.jcsr.2018.03.038.

[16] Braxtan NL, Pessiki SP. Postearthquake fire performance of sprayed fire-resistive material on steel moment frames. J Struct Eng 2011;137(9):946–53. https://doi.org/10.1061/(ASCE)ST.1943-541X.0000441.

[17] Keller WJ, Pessiki S. Effect of earthquake-induced damage to spray-applied fire-resistive insulation on the response of steel moment-frame beam-column connections during fire exposure. J Fire Prot Eng 2012;22(4):271–99. https://doi.org/10.1177/1042391512461126.

[18] Li VC. On engineered cementitious composites (ECC) a review of the material and its applications. J Adv Concr Technol 2003;1(3):215–30. https://doi.org/10.3151/jact.1.215.

[19] Li VC. Engineered cementitious composites (ECC)-tailored composites through micromechanical modelling; 1998.

[20] Li VC, Wang S, Cynthia Wu. Tensile strain-hardening behavior of polyvinyl alcohol engineered cementitious composite (PVA-ECC). Mater J 2001;98(6).

[21] Ding Y, Yu K, Li M. A review on high-strength engineered cementitious composites (HS-ECC): design, mechanical property and structural application. Struct Elsevier 2022;35:903–21. https://doi.org/10.1016/j.istruc.2021.10.036.

[22] Singh M, Saini B, Chalak HD. Performance and composition analysis of engineered cementitious composite (ECC) – a review. J Build Eng 2019;26:100851. https://doi.org/10.1016/j.jobe.2019.100851.

[23] Hou M, Zhang D, Li VC. Crack width control and mechanical properties of low carbon engineered cementitious composites (ECC). Constr Build Mater 2022;348:128692. https://doi.org/10.1016/j.conbuildmat.2022.128692.

[24] Sun R, Lu W, Ma C, et al. Effect of crack width and wet-dry cycles on the chloride penetration resistance of engineered cementitious composite (ECC). Constr Build Mater 2022;352:129030. https://doi.org/10.1016/j.conbuildmat.2022.129030.

[25] Wang T, Zhang D, Zhu H, et al. Durability and self-healing of engineered cementitious composites exposed to simulated sewage environments. Cem Concr Compos 2022;129:104500. https://doi.org/10.1016/j.cemconcomp.2022.104500.

[26] Liu H, Zhang Q, Li V, et al. Durability study on engineered cementitious composites (ECC) under sulfate and chloride environment. Constr Build Mater 2017;133:171–81. https://doi.org/10.1016/j.conbuildmat.2016.12.074.

[27] Rokugo K, Kanda T, Yokota H, et al. Applications and recommendations of high performance fiber reinforced cement composites with multiple fine cracking (HPFRCC) in Japan. Mater Struct 2009;42(9):1197–208. https://doi.org/10.1617/s11527-009-9541-8.

[28] Huang BT, Li QH, Xu SL, et al. Strengthening of reinforced concrete structure using sprayable fiber-reinforced cementitious composites with high ductility. Compos Struct 2019;220:940–52. https://doi.org/10.1016/j.compstruct.2019.04.061.

[29] Huang BT, Zhu JX, Weng KF, et al. Prefabricated UHPC-concrete-ECC underground utility tunnel reinforced by perforated steel plate: experimental and numerical investigations. Case Stud Constr Mater 2022;16:e00856. https://doi.org/10.1016/j.cscm.2021.e00856.

[30] Li Q, Yin X, Huang B, et al. Strengthening of the concrete face slabs of dams using sprayable strain-hardening fiber-reinforced cementitious composites. Front Struct Civ Eng 2022;16(2):145–60. https://doi.org/10.1007/s11709-022-0806-4.

[31] Li VC. Engineered cementitious composites (ECC): bendable concrete for sustainable and resilient infrastructure. Springer; 2019.

[32] Zhu JX, Xu LY, Huang BT, et al. Recent developments in engineered/strain-hardening cementitious composites (ECC/SHCC) with high and ultra-high strength. Constr Build Mater 2022;342:127956. https://doi.org/10.1016/j.conbuildmat.2022.127956.

[33] Zhang Q, Li VC. Adhesive bonding of fire-resistive engineered cementitious composites (ECC) to steel. Constr Build Mater 2014;64:431–9. https://doi.org/10.1016/j.conbuildmat.2014.04.059.

[34] Zhang Q, Li VC. Development of durable spray-applied fire-resistive engineered cementitious composites (SFR-ECC). Cem Concr Compos 2015;60:10–6. https://doi.org/10.1016/j.cemconcomp.2015.03.012.

[35] Zhang Q, Ranade R, Li VC. Feasibility study on fire-resistive engineered cementitious composites. ACI Mater J 2014;111(6):651–60.

[36] Cai Z, Liu F, Yu J, et al. Development of ultra-high ductility engineered cementitious composites as a novel and resilient fireproof coating. Constr Build Mater 2021;288:123090. https://doi.org/10.1016/j.conbuildmat.2021.123090.

[37] Cai Z, Yu J, Tian L, et al. Fire resistance of post-earthquake steel beams insulated with a novel fire-resistive coating-FR-ECC. Eng Struct 2021;246:112887. https://doi.org/10.1016/j.engstruct.2021.112887.

[38] Zhang Z, Yuvaraj A, Di J, et al. Matrix design of light weight, high strength, high ductility ECC. Constr Build Mater 2019;210:188–97. https://doi.org/10.1016/j.conbuildmat.2019.03.159.

[39] Yu K, Zhu H, Hou M, et al. Self-healing of PE-fiber reinforced lightweight high-strength engineered cementitious composite. Cem Concr Compos 2021;123:104209. https://doi.org/10.1016/j.cemconcomp.2021.104209.

[40] Zhou S, Xie L, Jia Y, et al. Review of cementitious composites containing polyethylene fibers as repairing materials. Polymers 2020;12(11):2624. https://doi.org/10.3390/polym12112624.

[41] Li Y, Tan KH, Yang EH. Synergistic effects of hybrid polypropylene and steel fibers on explosive spalling prevention of ultra-high performance concrete at elevated temperature. Cem Concr Compos 2019;96:174–81. https://doi.org/10.1016/j.cemconcomp.2018.11.009.

[42] Zhang D, Tan KH. Effect of various polymer fibers on spalling mitigation of ultra-high performance concrete at high temperature. Cem Concr Compos 2020;114:103815. https://doi.org/10.1016/j.cemconcomp.2020.103815.

[43] JC/T2461-2018. Test method for Mechanical Properties of High ductility Fiber-reinforced Cement Matrix Composites. Beijing: Building Materials Industry Press; 2018.

[44] SAC. Fire resistive coating for steel structure (GB 14907-2018), Standardization Administration of the People's Republic of China, Beijing; 2018.

[45] GB/T 32064-2015. Determination of thermal conductivity and thermal diffusivity of building materials: transient plane heat source method. Beijing: Beijing Zhongjian Architectural Science Research Institute Co. LTD; 2015.

[46] Xu S, Mu F, Wang J, et al. Experimental study on the interfacial bonding behaviors between sprayed UHTCC and concrete substrate. Constr Build Mater 2019;195:638–49. https://doi.org/10.1016/j.conbuildmat.2018.11.102.

[47] Kanda T, Saito T, Sakata N, Hiraishi M. Tensile and anti-spalling properties of direct sprayed ECC. J Adv Concr Technol 2003;1(3). https://doi.org/10.3151/jact.1.269.

[48] ISO 834-1. Fire-resistance tests-elements of building construction, Part 1: General Requirements. International Organization for Standardization. 1999: 1-25.